Available online at www.sciencedirect.com
SCIENCE DIRECT®
Journal of Electroanalytical Chemistry 573 (2004) 215–225
Journal of Electroanalytical Chemistry
www.elsevier.com/locate/jelechem

Electrogenerated chemiluminescence 73: acid–base properties, electrochemistry, and electrogenerated chemiluminescence of neutral red in acetonitrile

Jai-Pil Choi [1], Allen J. Bard *

Department of Chemistry and Biochemistry, The University of Texas at Austin, 1 University Station A5300, Austin, TX 787120165, USA

Received 10 February 2004; received in revised form 5 July 2004; accepted 7 July 2004
Available online 23 August 2004

Abstract

We characterized the acid–base properties, electrochemistry, and electrogenerated chemiluminescence (ECL) of neutral red in acetonitrile (MeCN). To determine the acid–base properties, the basic form (NR) of neutral red was prepared and titrated with anhydrous $HClO_4$, yielding $pK_a = 6.5$ in MeCN. NR showed three irreversible electrochemical oxidations and a one-electron reversible reduction. However, the acid form (NRH^+) was reduced at more positive potentials than NR in a two-electron transfer reaction. Benzoyl peroxide (BPO) was used as a co-reactant to generate ECL on reduction of NR because it produces a strong oxidizing agent ($C_6H_5CO_2^{\bullet}$) on reduction. A high concentration of BPO quenched ECL. NRH^+ did not produce ECL because its reduction was by the transfer of two electrons and the energy available in the ECL reaction was not sufficient to generate an excited state. However, the NR ECL showed a maximum intensity at 610 nm, which corresponds to the λ_{max} of NRH^+ fluorescence rather than that of NR. The ECL intensity of NR depended strongly on the concentration of NR, BPO, and trifluoroacetic acid (TFA). The integrated ECL intensity of NR, compared with that of $Ru(bpy)_3^{2+}$, yielded a relative ECL intensity ratio, $I_{NR}/I_{Ru(II)}$ of ~0.05.

Keywords: Neutral red; Tris(2,2′-bipyridine)ruthenium(II); Benzoyl peroxide; Electrogenerated chemiluminescence; Co-reactant; Quencher

1. Introduction

3-Amino-7-dimethylamino-2-methylphenazine, also known as neutral red, has been used in studies of biological systems, especially as an intracellular pH indicator [1,2], a nontoxic stain [3,4], and a probe material [5–7]. In aqueous solutions, neutral red is involved in an equilibrium between the protonated form (NRH^+) and a deprotonated form (NR), as shown below with a $pK_a = 6.81$ [8].

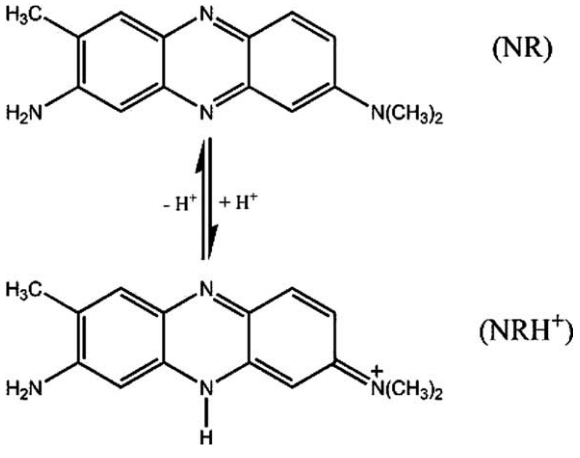

In addition, the electronic absorption spectra of neutral red in aqueous solutions show maximum absorption

* Corresponding author. Tel.: +1-512-471-3761; fax: +1-512-471-0088.
E-mail address: ajbard@mail.utexas.edu (A.J. Bard).
[1] Present address: Kenan Laboratories of Chemistry, University of North Carolina, Chapel Hill, NC 27599-3290, USA.

0022-0728/$ - see front matter © 2004 Elsevier B.V. All rights reserved.
doi:10.1016/j.jelechem.2004.07.007

peaks at 531 nm at low pH (e.g. pH 3.5) and at 450 nm at high pH (e.g. pH 10.5) [8]. A distinctive color change is observed at ~pH 7; the color of a neutral red solution changes from yellow to red as the solution changes from basic to acidic.

Electrogenerated chemiluminescence (ECL) is a phenomenon where an energetic electron transfer reaction of electrogenerated species produces the excited state usually with the regeneration of emitters [9–11]. In ECL, the excited state can be generated by either ion annihilation or use of a co-reactant. The ECL produced by ion annihilation usually requires the generation of both stable radical anions ($R^{\bullet -}$) and radical cations ($R^{\bullet +}$) by alternating or scanning the electrode potential. These two species can react to produce the excited state (R*) in the diffusion layer of an electrode, depending on the energy ($-\Delta H^\circ$) available in the ion annihilation reaction.

$$R^{\bullet -} + R^{\bullet +} \rightarrow 2R \ (\text{if} - \Delta H^\circ < E_s \text{ or } E_t) \quad (1)$$

$$R^{\bullet -} + R^{\bullet +} \rightarrow R^* + R \ (\text{if} - \Delta H^\circ > E_s \text{ or } E_t) \quad (2)$$

where R is an ECL emitter, E_s is the lowest excited singlet state energy, and E_t is the triplet state energy.

However, ECL can still be produced, even when one of the radical ions, $R^{\bullet -}$ or $R^{\bullet +}$, is either not produced or is unstable, in the presence of a co-reactant by pulsing or scanning the electrode potential in only one direction, either negative or positive. A co-reactant is a species that can produce a strong oxidizing or a reducing agent by an electrode reaction occurring with the electrochemical electron transfer (ET) reaction of the emitter precursor. For example, tris(2,2′-bipyridine)ruthenium(II), $Ru(bpy)_3^{2+}$ (bpy = 2,2′-bipyridine), can generate ECL in the presence of peroxydisulfate ion ($S_2O_8^{2-}$) by sweeping the potential only in the negative direction [12–14]. ECL has proven to be a versatile analytical technique with high sensitivity and selectivity and is used commercially for immunoassay [11,15,16]. Understanding ECL mechanisms and optimizing conditions for generating ECL are important in the application of ECL analytical methods and in developing new ECL emitters as labels and finding new co-reactants.

In this paper, we report how the ECL of NR [and $Ru(bpy)_3^{2+}$] is generated by use of a co-reactant, benzoyl peroxide (BPO) in acetonitrile (MeCN). The spectroscopic behavior and electrochemistry of NR and NRH^+ are also described.

2. Experimental

2.1. Chemicals

The hydrochloride form of neutral red (NR-HCl, high purity) was purchased from Acros (Houston, TX). NR was prepared from NR-HCl by dissolving 3 mg of NR-HCl in 50 mL deionized water, adding a saturated NaOH solution until a reddish-brown precipitate of NR formed, filtering this precipitate and washing it thoroughly with deionized water, and drying it in a vacuum oven at 70 °C for 24 h. Anhydrous MeCN, (99.93% in a sure-sealed bottle), trifluoroacetic acid (TFA, 99+ %), perchloric acid (70%, twice distilled), acetic anhydride (99.5%), glacial acetic acid (99.8%), tetra-*n*-butylammonium perchlorate (TBAP), and benzoyl peroxide (BPO) were obtained from Aldrich (Milwaukee, WI) and used as received. Anhydrous 1 M perchloric acid ($HClO_4$) in acetic acid was made by heating a solution of 70% aqueous $HClO_4$ (8.6 mL) in glacial acetic acid (72.4 mL) with acetic anhydride (19 mL) to a temperature of 70 °C for 8 h [17]. This stock solution was standardized by titration with potassium hydrogen phthalate (Aldrich, Milwaukee, WI) in acetic acid using crystal violet (Aldrich, Milwaukee, WI) as an indicator. TBAP and BPO were dried at 30 °C in a vacuum oven before being transferred to an inert atmosphere drybox (Vacuum Atmosphere Co., Hawthorne, CA).

2.2. Spectroscopy

Electronic absorption spectra were taken with a Beckman DU 640 spectrophotometer (Fullerton, CA). Fluorescence spectra were obtained with an ISA Spex Fluorolog-3 (JY Horiba, Edison, NJ). A quartz cuvette with a 1 cm path length was used for all spectroscopic measurements. All solutions used for absorption and fluorescence spectra were prepared in a drybox or purged with nitrogen (N_2) gas.

2.3. Electrochemistry

Electrochemical measurements were performed with either a CHI 660 electrochemical workstation (CH Instruments, Austin, TX) or a PAR model 173/175. For cyclic voltammetry, a conventional three-electrode electrochemical cell was used. A platinum (Pt) ultramicroelectrode (UME, 25 μm diameter) was used for steady-state voltammetry and a Pt disk electrode (2 mm diameter) was used for cyclic voltammetry and ECL. A Pt wire and a silver (Ag) wire were employed as the auxiliary electrode and the quasi-reference electrode (QRE), respectively. All electrode potentials were calibrated by using the ferrocene (Fc)/ferrocenium (Fc^+) redox couple and converted to V vs SCE by taking E° (Fc/Fc^+) = 0.424 V vs SCE [18]. All electrodes were polished with 0.05 μm alumina suspension (Buehler, Lake Bluff, IL), and sonicated in deionized water and ethanol. Then, all electrodes were dried in an oven at 120 °C for at least 20 min. Immediately after drying, they were transferred into the drybox.

2.4. Electrogenerated chemiluminescence

All ECL spectra were measured as previously reported [19]. A charge-coupled device (CCD) camera (Photometrics CH260, Tucson, AZ) cooled to −110 °C and interfaced to a computer was used to obtain ECL spectra. The CCD camera was focused on the exit slit of a grating spectrometer (concave grating) having a 1 mm entrance slit (Holographics, Inc.). For simultaneous cyclic voltammograms (CVs) and integrated ECL signals, a photomultiplier tube (PMT, Hamamatsu R4220p) was used, with −750 V supplied to the PMT with a high-voltage power supply series 225 (Bertan High Voltage Co., Hicksville, NY). All ECL spectra were produced by pulsing potentials from 0 V to the cathodic peak potential of NR and all integrated ECL signals were produced by sweeping potentials from 0 V to a potential sufficiently negative to generate the radical anion of NR.

3. Results and discussion

3.1. Acid–base properties of NR in MeCN

To characterize the acid–base properties of NR in MeCN, anhydrous $HClO_4$ in acetic acid was used as a titrant because it is completely dissociated in MeCN [20]. Fig. 1 shows the electronic absorption spectra of 10 μM NR titrated with anhydrous $HClO_4$ in MeCN. The acetic acid used for preparing an anhydrous $HClO_4$ stock solution did not interfere with the electronic absorption spectra of NR or contribute to the total concentration of H^+, because acetic acid is an extremely weak acid in MeCN [21]. Like electronic absorption spectra measured in aqueous solution, NR exhibited

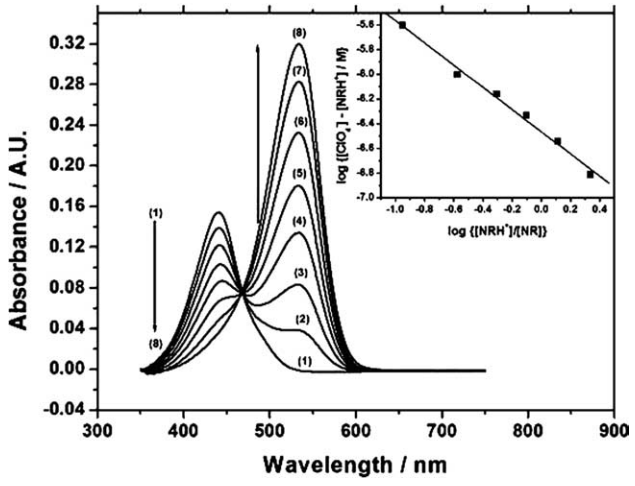

Fig. 1. Electronic absorption spectra of 10 μM NR titrated with (1) 0 μM, (2) 2 μM, (3) 3 μM, (4) 4 μM, (5) 5 μM, (6) 6 μM, (7) 7 μM, and (8) 10 μM of anhydrous $HClO_4$ in acetonitrile. Inset is a plot of $\log\{[ClO_4^-] - [NRH^+]\}$ vs $\log\{[NRH^+]/[NR]\}$.

one absorption band with a maximum intensity at 441 nm and the color of a 10 μM NR solution in MeCN was a bright yellow. As the concentration of $HClO_4$ increased, the intensity of the absorption band at 441 nm decreased and a new absorption band appeared with a maximum intensity at 533 nm. In addition, an isosbestic point was found at 468 nm, indicating that only two forms (NR and NRH^+) existed in equilibrium in MeCN. When 10 μM $HClO_4$ was added, the absorption band at 441 nm disappeared and the color of this solution became red.

The acid dissociation constant (K_a) for the acid–base reaction of NR

$$NR + H^+ \rightleftarrows NRH^+ \tag{3}$$

can be estimated from the electronic absorption spectra in Fig. 1 [20]. The equilibrium constant ($1/K_a$) for this reaction is:

$$\frac{1}{K_a} = \frac{[NRH^+]f_{NRH^+}}{[NR][H^+]f_{NR}f_{H^+}} \cong \frac{[NRH^+]}{[NR][H^+]} \tag{4}$$

where f represents the activity coefficient. In a dilute solution, f_{NRH^+} cancels out with f_{H^+} and f_{NR} is close to unity, because it is an uncharged species. Therefore, K_a is a function of concentration. Because $HClO_4$ is completely dissociated in MeCN, $[H^+]$ is:

$$[H^+] = [ClO_4^-] - [NRH^+] \tag{5}$$

or, with Eq. (4)

$$\log\{[ClO_4^-] - [NRH^+]\} = \log\frac{[NRH^+]}{[NR]} + \log K_a \tag{6}$$

$[NRH^+]$ and [NR] can be calculated from the absorption spectra by Beer's law and $[ClO_4^-]$ is the same as the concentration of $HClO_4$ added in the NR solution. Therefore, a plot of $\log\{[ClO_4^-] - [NRH^+]\}$ vs $\log\{[NRH^+]/[NR]\}$ should be linear (see inset of Fig. 1.) and the pK_a value of NR can be estimated from the y-intercept of that plot, yielding $pK_a = 6.5$ in MeCN.

3.2. Electrochemistry of NR and NRH^+

There have been several reports on the electrochemistry of neutral red in aqueous solution [22–24], mainly focused on the electrochemical reduction of NRH^+, but the electrochemistry of NR and NRH^+ in an organic solvent has not been previously reported, even though neutral red was first synthesized in 1878 [25]. Fig. 2 shows the CVs of 1 mM NR in MeCN containing 0.1 M TBAP at 0.1 V/s (Fig. 2(a)) and the scan rate dependence of peak potentials (E_p) and peak currents (i_p) for NR reduction (Fig. 2(b)). When the electrode potential was scanned towards positive potentials, three irreversible electrochemical oxidation waves were found at +0.74 V, +1.18 V, and +1.55 V vs SCE (see Fig. 2(a)). In contrast, the electrochemical reduction of NR was

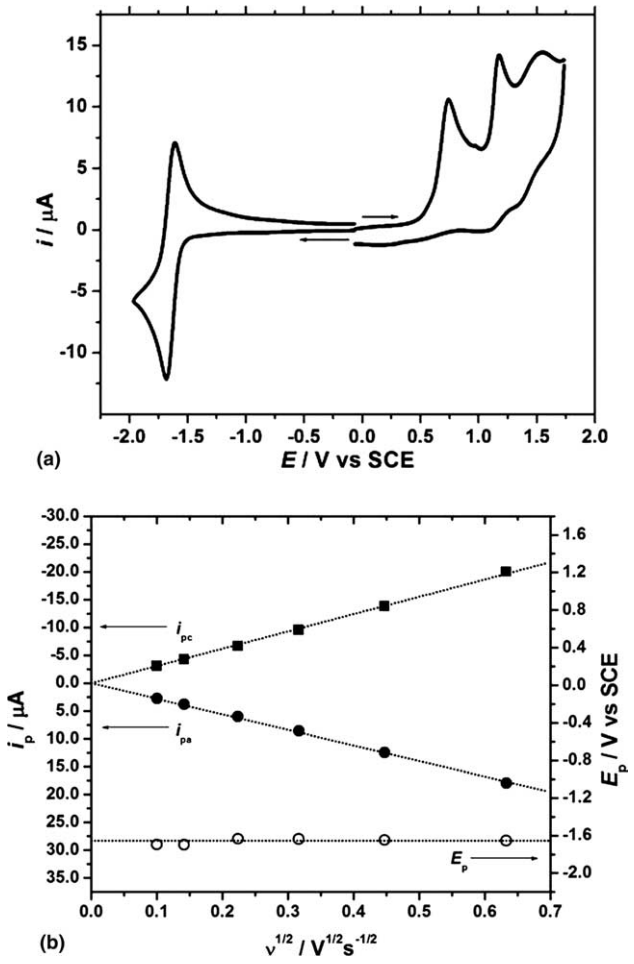

Fig. 2. (a) CVs of 1 mM NR in 0.1 M TBAP + MeCN at 0.2 V/s. (b) Dependence of peak potentials (E_p) and peak currents (i_{pc} and i_{pa}) of NR reduction on scan rate ($v^{1/2}$).

reversible with E_p-values independent of the scan rate (v) (see Fig. 2(b)) and the i_p ratio, i_{pa}/i_{pc}, where i_{pc} is the NR reduction current and i_{pa} is its corresponding oxidation current on scan reversal, was close to unity (~0.9). Both i_{pc} and i_{pa} were linearly dependent on $v^{1/2}$ indicating that this reduction is diffusion-controlled (see Fig. 2(b)), and the half-wave potential ($E_{1/2}$) of NR reduction was −1.64 V vs SCE. However, multiple scans from the positive (oxidation of NR) to the negative direction (reduction of NR) showed large changes in the CVs, implying that the radical cation of NR ($NR^{\cdot+}$) is unstable and decomposes.

The electrochemical reduction of NR was investigated with different concentrations of trifluoroacetic acid (TFA). Fig. 3 shows CVs for the electrochemical reduction of 1 mM NR in 0.1 M TBAP + MeCN with various concentrations of TFA at 0.1 V/s. As the concentration of TFA increased, the original reduction peak for NR at −1.47 V vs Ag QRE diminished and a new reduction wave, that of NRH^+, developed at a much more positive potential (with a 1.11 V shift). In addition, the i_ps for both reductions were linearly dependent on the concentration of TFA upto 1.8 mM (Fig. 4), with the i_p for NRH^+ becoming independent of the concentration of TFA above 2.2 mM TFA, where the original reduction peak for NR disappeared totally, because all of the NR molecules had been protonated by the TFA. H^+ reduction occurred at a more negative potential than the NRH^+ reduction potential. The i_p of NR in the absence of TFA was about half that for NRH^+ in 3 mM TFA, indicating that the n for the reduction of NRH^+ is different from that of NR (Fig. 4).

The diffusion coefficient (D) and the number of electrons transferred during the reduction (n) were estimated from the steady-state current and the chronoamperometric diffusion current (transient current) of a UME [26]. The steady-state current at a disk-shaped UME [27,28] is:

$$i_{ss} = 4nFDC^*a, \tag{7}$$

where F is Faraday's constant, C^* is the bulk concentration of analyte, and a is the radius of the UME. Because the current response at a UME having a radius a is the same as that of a hemisphere electrode having $r_s = 2a/\pi$ [29,30], the chronoamperometric diffusion current, $i_d(t)$, is given by:

$$i_d(t) = \pi^{1/2}nFD^{1/2}C^*a^2t^{1/2} + 4nFDC^*a \tag{8}$$

By normalizing Eq. (8) with Eq. (7), the normalized current, $i_d(t)/i_{ss}$ at a UME is:

$$i_d(t)/i_{ss} = (\pi^{1/2}/4)aDt^{-1/2} + 1 \tag{9}$$

Therefore, $i_d(t)/i_{ss}$ is a function of $t^{-1/2}$ and a plot of $i_d(t)/i_{ss}$ vs $t^{-1/2}$ should be linear, where D can be estimated from the slope and n can be calculated from the D value and known values of a and C^* from Eq. (7) [26].

Fig. 5(a) shows steady-state voltammograms of NRH^+ and NR reduction. Although i_{ss} was not well defined for NRH^+, because H^+ reduction begins to occur at the potentials on the plateau of the wave, it was still possible to approximate i_{ss} of NRH^+ reduction. The measured i_{ss} s were 9.9 nA for NRH^+ and 4.7 nA for NR. Fig. 5(b) and (c) are the plots of $i_d(t)/i_{ss}$ vs $t^{-1/2}$ for NR and NRH^+, respectively. In the short time region ($t < 1$ ms), the experimental data points deviate from linearity because of double layer charging, the finite rise time of the potentiostat and current follower, and perhaps finite heterogeneous electron transfer kinetics. For the longer time region, however, $i_d(t)/i_{ss}$ was a linear function of $t^{-1/2}$ and its slope was extracted by a linear regression. The calculated slopes of 0.180 for NR and 0.182 for NRH^+ yield D values of 9.5×10^{-6} and 9.3×10^{-6} cm^2/s, respectively. The n values calculated from Eq. (7) were 1.02 for NR and 2.20 for NRH^+, as summarized in Table 1.

The proposed electrochemical reduction mechanism for NR and NRH^+ is a "square scheme" as shown in Scheme 1. Because NR is a derivative of phenazine, its

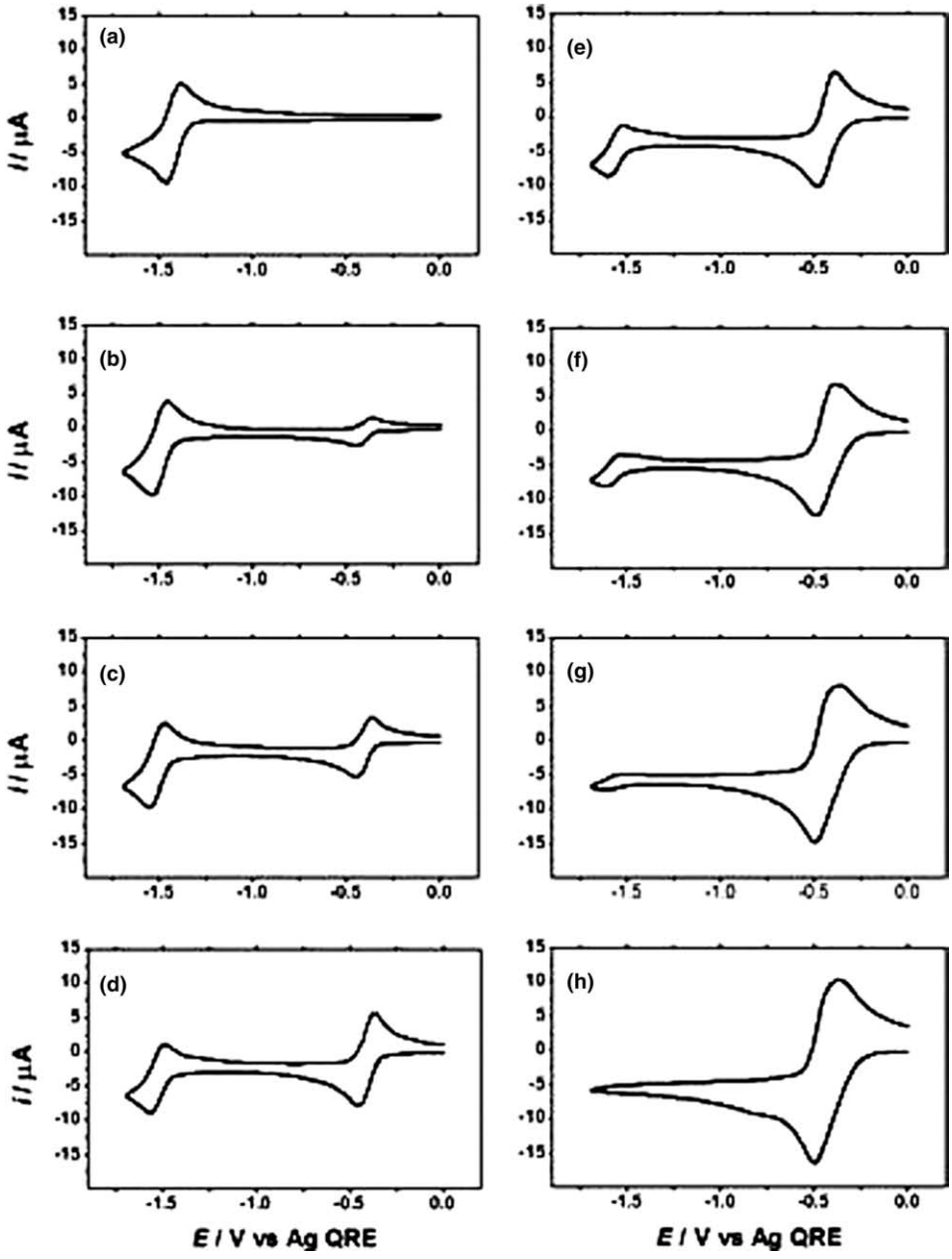

Fig. 3. CVs of 1 mM NR titrated with (a) 0 mM, (b) 0.26 mM, (c) 0.52 mM, (d) 0.78 mM, (e) 1.04 mM, (f) 1.30 mM, (g) 1.56 mM, and (h) 1.82 mM trifluoroacetic acid (TFA) in 0.1 M TBAP + MeCN at 0.1 V/s.

electrochemical reduction mechanism should be similar to that of phenazine [31]. Therefore, two successive one-electron reductions of NR occur (paths (a) and (b) in Scheme 1). Similarly, NRH^+ is reduced in an ECE process leading to an overall two-electron reaction. Similar phenomena were observed in the electrochemical reduction of phenazine and protonated phenazine in DMF or DMSO [31].

3.3. ECL of NR

No ECL by ion annihilation was observed by cycling between the anodic and cathodic waves of either NR, probably because of the instability of the radical cation. However, because NR produces a stable radical anion, a co-reactant that produces a strong oxidizing agent on reduction can generate ECL and BPO was used for this purpose.

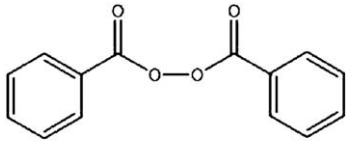

BPO

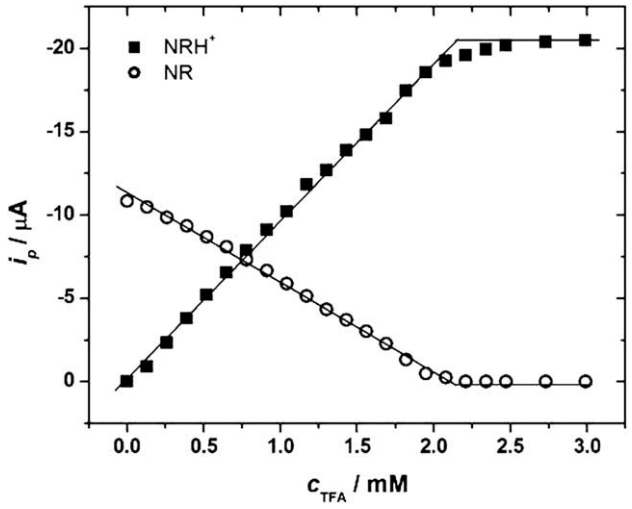

Fig. 4. Dependence of reduction peak currents (i_p) of NR and NRH^+ on the concentration of TFA in 0.1 M TBAP + MeCN. 1 mM NR was titrated with 0.13 M TFA stock solution. Scan rate = 0.1 V/s.

When BPO is reduced electrochemically, it produces a strong oxidizing agent, benzoate radical ($C_6H_5CO_2^{\bullet}$) [32], via an ECE process [33]. (vide infra)

$$BPO + e^- \rightarrow BPO^{\bullet -} \quad (10)$$

$$BPO^{\bullet -} \rightarrow C_6H_5CO_2^{\bullet} + C_6H_5CO_2^{\bullet -} \quad (11)$$

$$C_6H_5CO_2^{\bullet} + e^- \rightarrow C_6H_5CO_{2^-} \quad (12)$$

Fig. 6 shows the simultaneous CV (a) and ECL response (b) of a 1 mM NR + 5 mM BPO system in MeCN containing 0.1 M TBAP at 0.1 V/s. From the CV, BPO is seen to reduce at −1.25 V vs Ag QRE prior to NR reduction and no ECL was found at this potential, indicating that no luminescence was produced during BPO reduction alone. When the electrode potential reached the reduction potential of NR, ECL emission from NR was detected.

The proposed ECL mechanism of NR generated with BPO is shown in Scheme 2.

The generated $C_6H_5CO_2^{\bullet}$ is a sufficiently strong oxidizing agent to form an excited state of NR. However the $E^{\circ}(C_6H_5CO_2^{\bullet}/C_6H_5CO_2^{-})$ was reported to be either +0.8 V [34] or +1.5 V vs SCE [35]. Once NR is reduced (Eq. (13)), $C_6H_5CO_2^{\bullet}$ oxidizes $NR^{\bullet -}$ to NR* (Eq. (14)). To check the energetic feasibility for this reaction, the energy, $-\Delta H^{\circ}$ [36], available in Eq. (14) was estimated from Eq. (16) using $E_{1/2}$ ($NR/NR^{\bullet -}$) and E° ($C_6H_5CO_2^{\bullet}/C_6H_5CO_2^{-}$), and compared with the lowest excited singlet state energy (E_s) of NR, which was determined from the fluorescence spectrum of NR.

$$-\Delta H^{\circ} \approx E^{\circ}(C_6H_5CO_2^{\bullet}/C_6H_5CO_2^{-}) - E_{1/2}(NR/NR^{\bullet -}) - 0.1\ \text{eV} \quad (16)$$

where 0.1 eV is an estimate of the temperature-entropy approximation term ($T\Delta S^{\circ}$) at 25 °C. $-\Delta H^{\circ}$ for Eq.

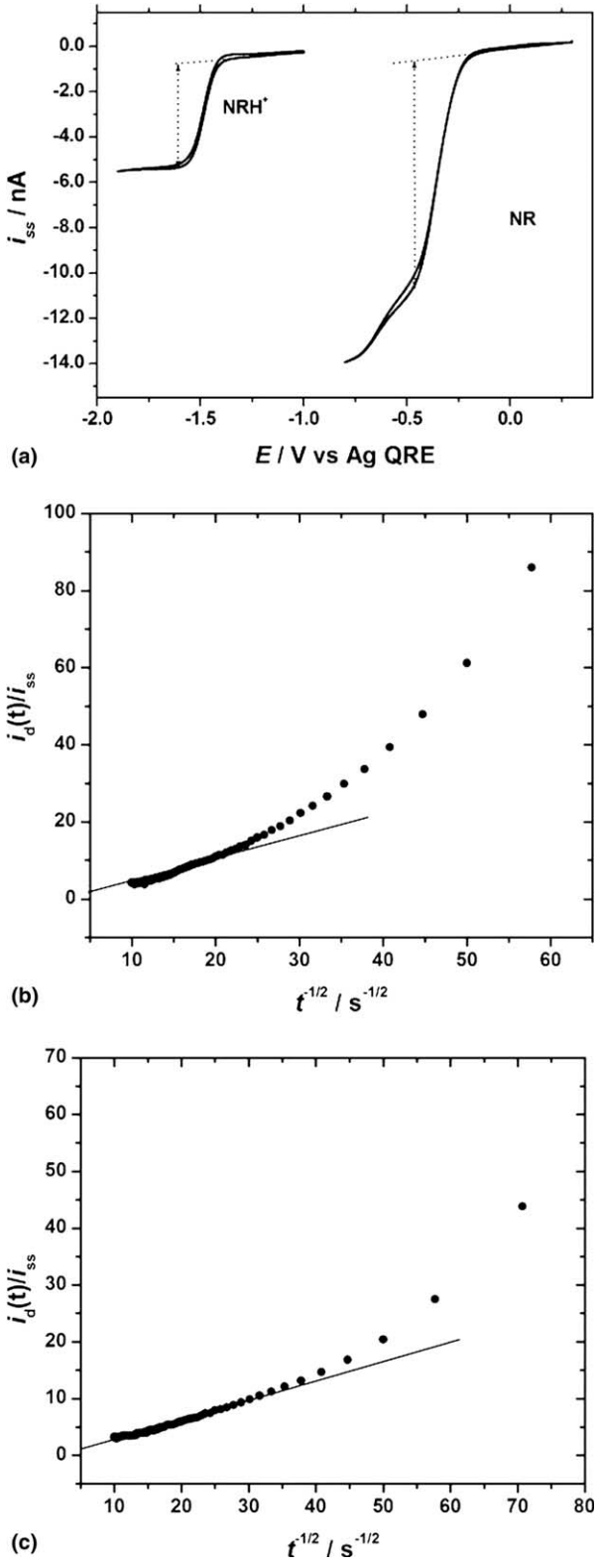

Fig. 5. (a) CVs of 1 mM NR and NRH^+ produced by adding 2 mM TFA in 1 mM NR, 0.1 M TBAP + MeCN at 10 mV/s using a Pt-UME (12.5 μm radius) working electrode. (b) and (c) Plots of the normalized current ratio, $i_d(t)/i_{ss}$ vs the inverse square root of time for reductions of 1 mM NR and 1 mM NRH^+, respectively, in 0.1 M TBAP + MeCN. Sampling rate, 100 s per point. A Pt-UME (12.5 μm radius) was used.

Table 1
Summary of $E_{1/2}$, n, and D for the Reductions of NR and NRH^+

	$E_{1/2}$ (V) vs SCE	n	10^6 D (cm^2 s^{-1})
NR	−1.64	1.02	9.5
NRH^+	−0.53	2.20	9.3

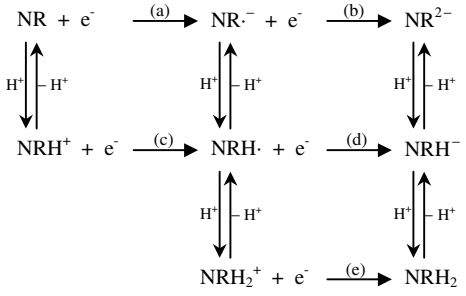

Scheme 1.

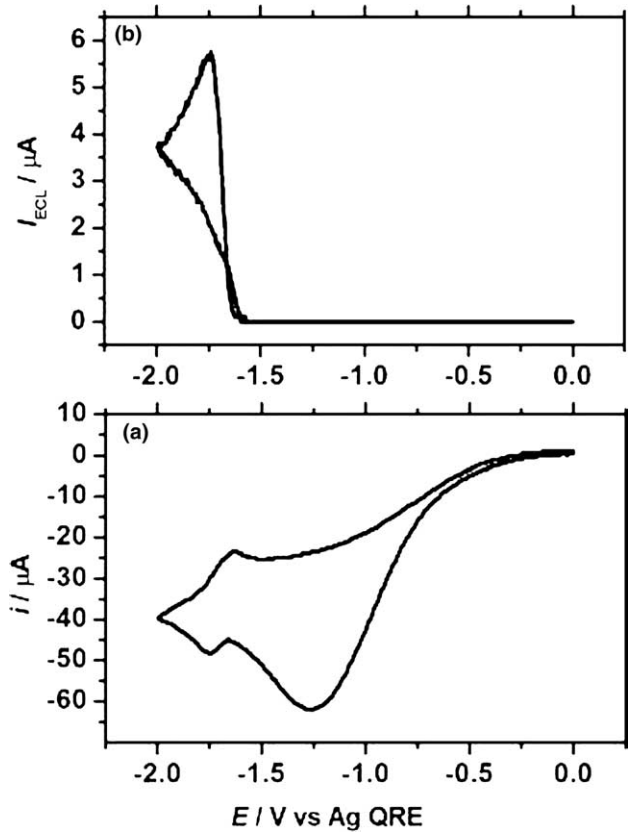

Fig. 6. Simultaneous (a) CV and (b) ECL signal of 1 mM NR produced with 5 mM BPO in 0.1 M TBAP + MeCN at 0.1 V/s.

(14) is 2.34 eV estimated with the lower E° value of benzoate radical, +0.8 V ($-\Delta H^\circ$ = 3.04 eV if E° = +1.5 V). Because $-\Delta H^\circ$ is larger than E_s of NR, the direct generation of NR* is possible. In contrast, no ECL signal was obtained with the NRH^+/BPO system. Because the electrochemical reduction of NRH^+ is a two-electron transfer reaction and $-\Delta H^\circ$ (1.93 eV) estimated even

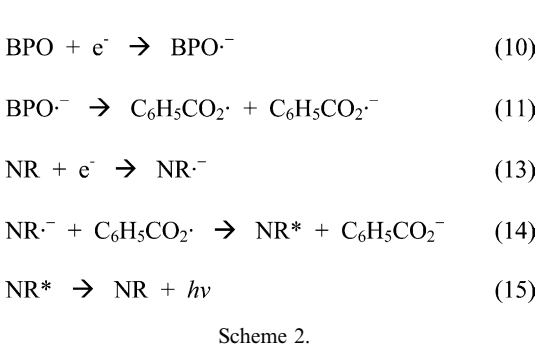

Scheme 2.

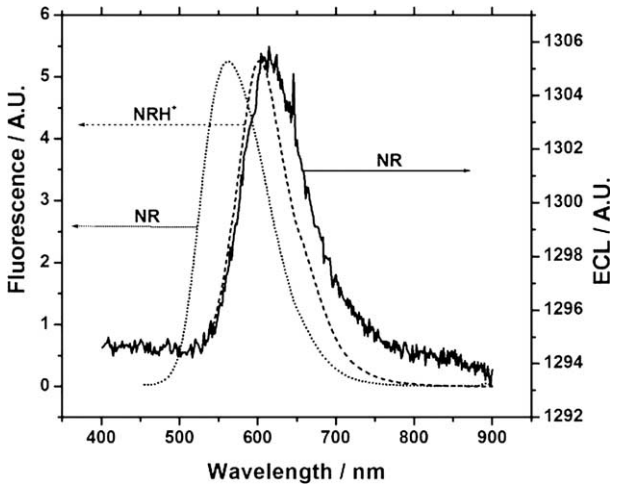

Fig. 7. ECL spectrum (solid line) of 1 mM NR and fluorescence spectra of 5 μM NR (dotted line) and 5 μM NRH^+ (dashed line). ECL was generated with 10 mM BPO by pulsing the electrode potential between 0 V and −1.6 V vs Ag QRE (0.1 s pulse width and 5 min integration). λ_{ex} for NR and NRH^+, 440 and 530 nm, respectively.

with the larger E° (+1.5 V) is less than E_s (2.06 eV) of NRH^+, it is energetically unfavorable to generate NRH^{+*} directly.

To determine that the observed ECL was emitted from NR, ECL spectra were measured with a CCD camera and compared with its fluorescence spectra. Fig. 7 shows the ECL spectrum of 1 mM NR produced with 10 mM BPO and the fluorescence spectra of 5 μM NR and 5 μM NRH^+. For this ECL spectrum, ECL was generated by pulsing the electrode potential between 0 V and −1.6 V vs QRE with 0.1 s pulse width for 5 min. The fluorescence maxima of NR and NRH^+ were found at 561 and 601 nm, respectively. Interestingly, the observed ECL spectrum of NR, which had a maximum intensity at 610 nm, corresponded more closely to the fluorescence of NRH^+ rather than that of NR. Although Singh et al. [37] reported the dual solvatochromism of NR in fluorescence and suggested the existence of two closely spaced electronic excited states, it is still not clear why ECL produces longer wavelength emission than does fluorescence, even in the same solvent.

Another possibility is the presence of unknown fluorescing species produced during the ECL reaction. To

test this, absorbance and fluorescence measurements were carried out again with the solution used for ECL, as soon as the ECL measurement was finished. The resulting absorption and fluorescence spectra were identical to those measured before ECL experiments, suggesting that no emissive bulk by-product was produced during the ECL reaction.

3.4. Concentration effects on ECL of NR

The ECL of NR depended strongly on the concentration of NR, H^+, and BPO. Fig. 8 shows the effect of NR concentration on the ECL produced with 5 mM BPO. The total ECL emission was measured with a PMT by scanning the electrode potential. The measured ECL intensity was linearly proportional to NR concentration upto 0.25 mM. However, the apparent ECL of NR gradually decreased in the range of 0.5–2 mM because of an inner-filter effect (self-absorption) and self-quenching at such high concentrations. Generally, the inner-filter effect occurs at longer path lengths when the wavelength of emission overlaps an absorption band and becomes significant with an increasing concentration of emitter. The rate of self-quenching, a bimolecular process, also increases with increasing concentration.

The ECL intensity of NR was also strongly dependent on the concentration of H^+ because the protonated form of NR does not produce ECL. Fig. 9 shows the effect of H^+ concentration on ECL of 1 mM NR using TFA as a H^+ donor. As shown in Fig. 9, the ECL intensity of NR was affected dramatically by a small amount of acid. The decay of the ECL intensity with added TFA is also caused by the inner-filter effect of the NRH^+ formed. Because the absorption band (λ_{max} = 533 nm) of NRH^+ is located more closely to the ECL band (λ_{max} = 610 nm) than that (λ_{max} = 441 nm) of NR, the inner-filter effect with NRH^+ is more important than with NR. In fact, a larger portion of the NRH^+ absorption band (15.8%) overlapped the NR ECL spectrum than did NR (2.8%).

Fig. 10 shows the ECL intensity of 0.5 mM NR as a function of the BPO concentration. The ECL intensity of 0.5 mM NR was linearly proportional to the concentration of BPO upto 10 mM. After that, the ECL intensity decreased with increasing BPO concentration, suggesting that NR* is quenched by BPO at high concentration. BPO proved to be an effective quencher for

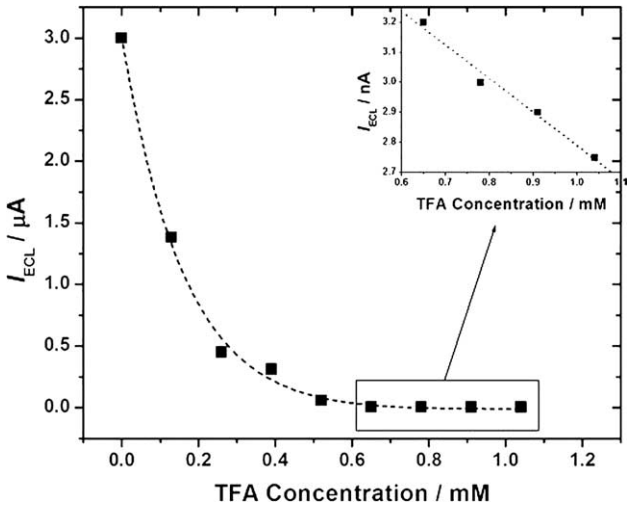

Fig. 9. Effect of TFA concentration on ECL of 1 mM NR produced with 5 mM BPO in 0.1 M TBAP + MeCN, with the electrode potential scanned at 0.1 V/s and measured with a PMT.

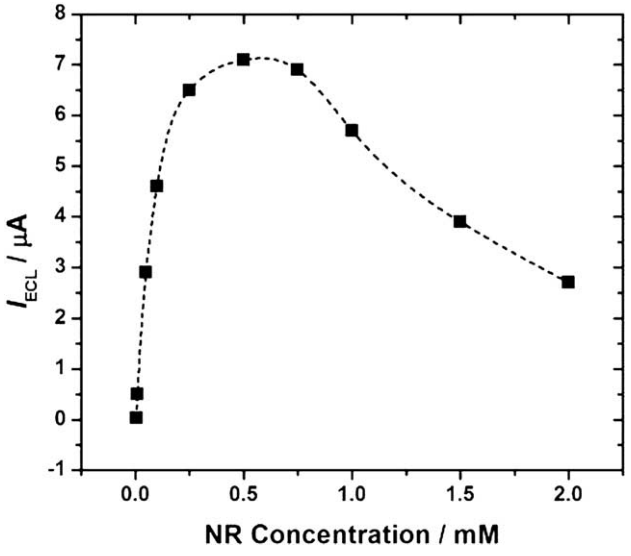

Fig. 8. Effect of NR concentration on ECL with 5 mM BPO in 0.1 M TBAP + MeCN, with the electrode potential scanned at 0.1 V/s and measured with a PMT.

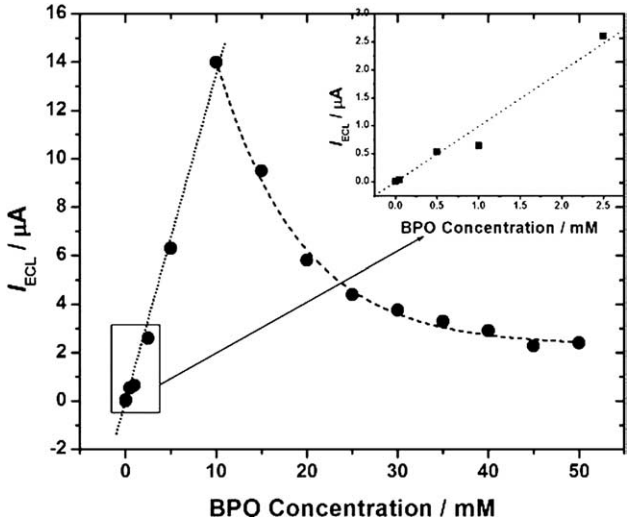

Fig. 10. Effect of BPO concentration on 0.5 mM NR in 0.1 M TBAP + MeCN, with the electrode potential scanned at 0.1 V/s and measured with a PMT. Inset represents the low concentration region (0–2.5 mM BPO).

the fluorescence of $Ru(bpy)_3^{2+}$ and some aromatic hydrocarbons [38,39]. In a similar way, ECL quenching might occur by electron transfer (ET) as follows:

$$NR^* + BPO \xrightarrow{k_q} [NR^{\bullet+} \cdots BPO^-] \quad (17)$$

$$[NR^{\cdot+} \ldots BPO^-] \rightarrow NR^{\cdot+} + C_6H_5CO_2^{\cdot} + C_6H_5CO_2^- \quad (18)$$

$$[NR^{\cdot+} \ldots BPO^-] \rightarrow NR + BPO \quad (19)$$

Once the intermediate state, $[NR^{\cdot+} \cdots BPO^-]$, was formed, both a decomposition reaction (Eq. (18)) and a back ET reaction (Eq. (19)) could occur. ECL quenching of 0.5 mM NR by BPO seemed not to be efficient at concentrations lower than 10 mM BPO.

Fluorescence quenching experiments were performed to confirm that BPO is a quencher of NR fluorescence. The fluorescence quenching rate constant (k_q) can be estimated from the Stern–Volmer relationship [40] in the absence of other quenchers, like molecular oxygen, as defined by:

$$\frac{I_0}{I} = 1 + K_{SV}[BPO] = 1 + k_q \tau^s [BPO], \quad (20)$$

where I and I_0 denote the fluorescence intensity with BPO and the initial fluorescence intensity without BPO, respectively, K_{SV} is the Stern–Volmer quenching constant, k_q is the quenching rate constant, and τ^s is the lifetime of the lowest excited singlet state. Fig. 11 shows the Stern–Volmer plot of NR fluorescence quenching. From the slope of this plot, K_{SV} and k_q were calculated as 6.9 M^{-1} and 1.6×10^9 $M^{-1}\,s^{-1}$, respectively, by taking τ^s as 4.2 ns [37].

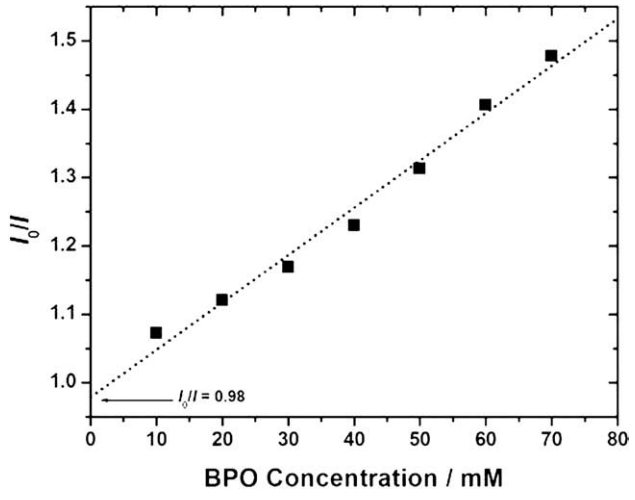

Fig. 11. Stern–Volmer plot of NR fluorescence quenching by BPO in the absence of molecular oxygen. c_{NR} = 1 μM and λ_{ex} = 440 nm.

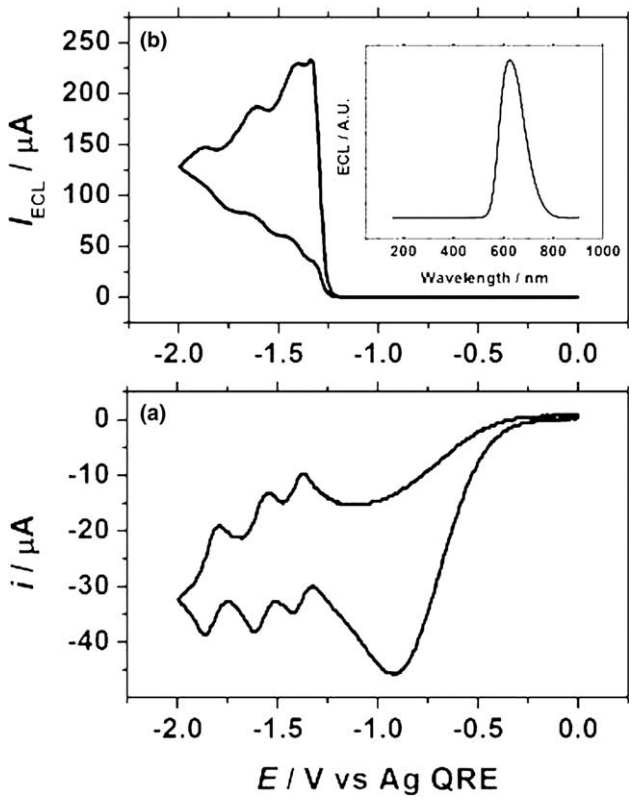

Fig. 12. Simultaneous (a) CV and (b) ECL wave of 1 mM $Ru(bpy)_3^{2+}$ and 5 mM BPO in 0.1 M TBAP + MeCN at 0.1 V/s. Inset of (b) represents the ECL spectrum measured under the same condition.

3.5. ECL of $Ru(bpy)_3^{2+}$ with BPO and ECL efficiency

BPO was also used to generate the cathodic ECL of $Ru(bpy)_3^{2+}$, which is a well known ECL emitter. Fig. 12 shows simultaneous CV (a) and ECL (b) curves of 1 mM $Ru(bpy)_3^{2+}$ produced with 5 mM BPO in 0.1 M TBAP + MeCN. When the electrode potential was scanned in the negative direction, BPO was reduced first. As with NR ECL, no luminescence occurred until $Ru(bpy)_3^{2+}$ was reduced. Three reversible reductions producing $Ru(bpy)^+$, $Ru(bpy)^0$, and $Ru(bpy)^-$ were observed at −1.42, −1.61, and −1.88 V vs Ag QRE, respectively (Fig. 12(a)), and ECL having a maximum intensity at 623 nm was produced (inset of Fig. 12(b)). Although ECL was also produced at the potential where $Ru(bpy)_3^0$ and $Ru(bpy)_3^+$ were generated, only the first ECL produced at the potential of the $Ru(bpy)^{2+/+}$ couple

Equations (10) and (11) followed by

$$Ru(bpy)_3^{2+} + e^- \rightarrow Ru(bpy)_3^+ \quad (21)$$

$$Ru(bpy)_3^{2+} + C_6H_5CO_2\cdot \rightarrow Ru(bpy)_3^{2+*} + C_6H_5CO_2^- \quad (22)$$

Scheme 3.

Equations (10), (11) and (21) with

$$Ru(bpy)_3^{2+} + C_6H_5CO_2^{\bullet} \rightarrow Ru(bpy)_3^{3+} + C_6H_5CO_2^{-} \quad (23)$$

$$Ru(bpy)_3^{+} + Ru(bpy)_3^{3+} \rightarrow Ru(bpy)_3^{2+*} + Ru(bpy)_3^{2+} \quad (24)$$

Scheme 4.

will be considered for the proposed ECL mechanism shown in Scheme 3.

The energy available in Eq. (22) can be estimated from Eq. (16) by replacing $E_{1/2}$ ($NR/NR^{\bullet -}$) with $E_{1/2}$ ($Ru(bpy)_3^{2+/+}$). The estimated $-\Delta H^{\circ}$ for Eq. (22) is at least 2.2 eV, which is greater than the excited state energy of $Ru(bpy)_3^{2+}$ (2.12 eV [41]). If $E^{\circ}(C_6H_5CO_2^{\bullet}/C_6H_5CO_2^{-})$ is taken as +1.5 V, an additional mechanism is also possible as shown in Scheme 4.

Eq. (23) can occur because $C_6H_5CO_2^{\bullet}$ (if E° = +1.5 V) is strong enough to oxidize $Ru(bpy)_3^{2+}$ (E° = 1.29 V [41]). Therefore, $Ru(bpy)_3^{2+*}$ can be produced via Eq. (24) as well as by Eq. (22) in Scheme 3.

In general, the ECL efficiency (ϕ_{ECL}) is defined as photons emitted per redox event that is related to the total electrical charge applied. Estimating the efficiency is possible only in annihilation ECL, where one can account for the charge in the generation of reactants. In co-reactant ECL, like the NR/BPO system, ϕ_{ECL} cannot be estimated, because the total charge does not represent the number of redox reactions between $NR^{\bullet -}$ and $C_6H_5CO_2^{\bullet}$. Therefore, the integrated ECL intensity of NR with BPO was compared with that of a reference, $Ru(bpy)_3^{2+}$, whose ϕ_{ECL} for annihilation is well known as ~5% [42–44], with BPO. Instead of ϕ_{ECL} we report the relative ECL intensity ratio ($I_{NR}/I_{Ru(II)}$) measured under the same conditions (0.5 mM NR + 10 mM BPO and 0.5 mM $Ru(bpy)_3^{2+}$ + 10 mM BPO), which is ~0.05.

4. Conclusions

Based on the property of color change depending on $[H^+]$, neutral red may be used as an acid–base indicator (pK_a = 6.5) in MeCN. In electrochemistry, both NR and NRH^+ did not show reversible oxidations in MeCN. However, reversible electrochemical reductions of NR (n = 1) and NRH^+ (n = 2) occur in MeCN. ECL of NR can be generated by using a co-reactant, BPO, which produces a strong oxidizing agent, $C_6H_5CO_2^{\bullet}$. However, NRH^+ does not generate ECL, because of its two-electron reduction and a lack of sufficient energy to produce the excited state. The ECL intensity of NR is strongly affected by the concentrations of NR itself, BPO, and H^+. The relatively high concentration of BPO quenches both ECL and fluorescence. The optimum condition for NR to produce ECL is 0.5 mM NR with 10 mM BPO in the absence of H^+ and molecular oxygen. The ECL efficiency is only about 5% of that of $Ru(bpy)_3^{2+}$ under the same conditions.

Acknowledgements

Support from IGEN Inc. and the Texas Advanced Research Program (0103) is gratefully acknowledged.

References

[1] J.C. Lumanna, K.A. McCracken, Anal. Biochem. 142 (1984) 117.
[2] M. Haumann, W. Junge, Biochemistry 33 (1994) 864.
[3] R. Osborne, M.A. Perkins, Food Chem. Toxicol. 32 (1994) 133.
[4] J.M. Gaullier, M. Geze, R. Santus, T. Sae Melo, J.C. Maziere, M. Bazin, P. Morliere, L. Dubertret, Photochem. Photobiol. 62 (1995) 114.
[5] K.W. Woodburn, N.J. Vardaxis, J.S. Hill, A.H. Kaye, D.R. Phillips, Photochem. Photobiol. 54 (1991) 725.
[6] G. Chen, C.L. Hanson, T.J. Ebner, Neurophysiol. 76 (1996) 4169.
[7] D. Okada, J. Neurosci. Meth. 101 (2000) 85.
[8] F.G. Walz Jr., B. Terenna, D. Rolince, Biopolymers 14 (1975) 825.
[9] L.R. Faulkner, R.S. Glass, in: W. Adam, G. Cilento (Eds.), Chemical and Biological Generation of Excited States, Academic Press, New York, 1982, Chapter 6.
[10] A.J. Bard (Ed.), Electrogenerated Chemiluminescence, Marcel Dekker, New York, 2004.
[11] A.J. Bard, J.D. Debad, J.K. Leland, G.B. Sigal, J.L. Wilbur, J.N. Wohlstadter, in: R.A. Meyer (Ed.), Encyclopedia of Analytical Chemistry: Applications, Theory, and Instrumentation, Wiley, New York, 2000, p. 9842.
[12] H.S. White, A.J. Bard, J. Am. Chem. Soc. 104 (1982) 6891.
[13] F. Bolleta, M. Ciano, V. Balzani, N. Serpone, Inorg. Chim. Acta 62 (1982) 207.
[14] W.G. Becker, H.S. Seung, A.J. Bard, J. Electroanal. Chem. 167 (1984) 127.
[15] A.J. Bard, G.M. Whitesides, US Patents 5 221 605 (1993), 5 238 808 (1993), and 5 310 687 (1994).
[16] G.F. Blackburn, H.P. Shah, J.H. Kenien, J. Leland, R.A. Kamin, J. Link, J. Peterman, M.J. Powell, A. Shah, D.B. Talley, S.K. Tyagi, E. Wilkins, T.-G. Wu, R.J. Massey, J. Clin. Chem. 37 (1991) 1534.
[17] E.K. Plyler, E.S. Barr, J. Chem. Phys. 2 (1935) 679.
[18] J.D. Debad, J.S. Morris, P. Magnus, A.J. Bard, J. Org. Chem. 62 (1997) 530.
[19] P. McCord, A.J. Bard, J. Electroanal. Chem. 318 (1991) 91.
[20] I.M. Kolthoff, S. Bruckenstein, M.K. Chantooni, J. Am. Chem. Soc. 83 (1961) 3927.
[21] J.F. Coetzee, I.M. Kolthoff, J. Am. Chem. Soc. 79 (1957) 6110.
[22] C.S. Halliday, D.B. Matthews, Aust. J. Chem. 36 (1983) 507.
[23] J.M. Bauldreay, M.D. Archer, Electrochim. Acta 28 (1983) 1515.
[24] S.E. Creager, G.T. Marks, D.A. Aikens, H.H. Richtol, J. Electroanal. Chem. 152 (1983) 197.
[25] E. Witt, Ber. Deutsch. Chem. Ges. 12 (1878) 931.
[26] G. Denuault, M.V. Mirkin, A.J. Bard, J. Electroanal. Chem. 308 (1991) 27.
[27] R.M. Wightman, D.O. Wipf, in: A.J. Bard (Ed.), Electroanalytical Chemistry, vol. 15, 1988, p. 267.

[28] A.J. Bard, F.-R. Fan, J. Kwak, O. Lev, Anal. Chem. 61 (1989) 132.
[29] K.B. Oldham, J. Electroanal. Chem. 122 (1981) 1.
[30] K.B. Oldham, C.G. Zoski, J. Electroanal. Chem. 256 (1988) 11.
[31] D.T. Sawyer, R.Y. Komai, Anal. Chem. 44 (1972) 715.
[32] J.-P. Choi, K.T. Wong, Y.-M. Chen, J.-K. Yu, P.-T. Chou, A.J. Bard, J. Phys. Chem. B 107 (2003) 14407.
[33] A.J. Bard, L.R. Faulkner, Electrochemical Methods, second ed., Wiley, New York, 2001, Chapter 12.
[34] D.L. Akins, R.L. Birke, Chem. Phys. Lett. 29 (1974) 428.
[35] E.A. Chandross, F.I. Sonntag, J. Am. Chem. Soc. 88 (1966) 1089.
[36] L.R. Faulkner, A.J. Bard, in: A.J. Bard (Ed.), Electroanalytical Chemistry, vol. 10, Marcel Dekker, New York, 1977, p. 1.
[37] M.K. Singh, H. Pal, A.C. Bhasikuttan, A.V. Sapre, Photochem. Photobiol. 68 (1998) 32.
[38] S. Oishi, K. Tajime, I. Shiojima, J. Mol. Catal. 14 (1982) 383.
[39] T. Urano, A. Kitamura, H. Sakuragi, K. Tokumaru, J. Photochem. 26 (1984) 69.
[40] F. Wilkinson, in: G.G. Guilbault (Ed.), Fluorescence: Theory, Instrumentation, and Practice, Marcel Dekker, New York, 1967, Chapter 1.
[41] K. Kalyanasundaram, Coord. Chem. Rev. 46 (1982) 159.
[42] N.E. Tokel-Takvoryan, R.E. Hemingway, A.J. Bard, J. Am. Chem. Soc. 95 (1973) 6582.
[43] W.L. Wallace, A.J. Bard, J. Phys. Chem. 83 (1979) 1350.
[44] J.D. Luttmer, A.J. Bard, J. Phys. Chem. 85 (1981) 1155.